Structural Engineering and Mechanics, Vol. 23, No. 4 (2006) 431-447
DOI: http://dx.doi.org/10.12989/sem.2006.23.4.431

An incremental convex programming model of the elastic frictional contact problems

S. A. Mohamed†, M. M. Helal‡ and F. F. Mahmoud‡†

Faculty of Engineering, Zagazig University, Zagazig, Egypt

(Received February 24, 2005, Accepted March 20, 2006)

Abstract. A new incremental finite element model is developed to simulate the frictional contact of elastic bodies. The incremental convex programming method is exploited, in the framework of finite element approach, to recast the variational inequality principle of contact problem in a discretized form. The non-classical friction model of Oden and Pires is adopted, however, the friction effect is represented by an equivalent non-linear stiffness rather than additional constraints. Different parametric studies are worked out to address the versatility of the proposed model.

Keywords: contact mechanics; friction; variational inequality; finite elements; convex programming; incremental approach.

1. Introduction

Friction between deformable bodies can be viewed as an additional resistance to relative sliding motion. This type of resistance is mainly depending on the applied normal load, relative material properties, quality and treatment of the mating surfaces. The classic laws of static dry friction as they evolved from early studies by Amonotons, Coulomb and others, asserts that only macro level sliding between two bodies in contact, will occur once the applied tangential force reaches a critical value. This tangential force is proportional to the net normal force, pressing the two bodies together, and independent of the apparent contact area. Those classical laws are eventually capable to describe only the friction effects between rigid bodies. Several friction theories have been proposed in the last five decades to explain the nature of dry friction between the surfaces of deformable bodies and accordingly, most of the laws of classical friction theory developed by Coulomb have been found to be incorrect. The friction physical model, proposed by Bowden and Tabor (1950), is now widely accepted for metal friction. The model states that once the normal load is applied on the two contacting bodies high pressure will be developed at individual contact spots and causing local welding. The junctions thus formed by welding are subsequently sheared by any relative sliding of the two surfaces. Ploughing by asperities of the harder surface through the matrix of the softer material contribute an additional component of friction. Accordingly we may assume that the

† Associate Professor
‡ Assistant Professor
‡† Professor, Corresponding author, E-mail: faheem@aucegypt.edu

evolved friction force consists of two independent components, adhesion component, due to the welding of the junctions, and grooving component, due to the ploughing of asperities. In most cases, the ploughing term is insignificant and we can assume that the adhesion component contributing only the entire friction resistance to motion.

The welding-ploughing theory implies that by increasing the capacity of the monotonic tangential force, the welded junctions of asperities start compliance gradually until A complete fracture of all junctions occurs, causing a macro slip motion. Therefore, the state of motion is switched from quasi-static to rigid body motion.

In the present paper, we adopt the adhesion-ploughing theory to propose a non-classical friction model (section 2). This model is similar to that developed by Oden and Pires (1983). In section 3 we present the variational inequality formulation of the frictional Signorini's problem. The proposed friction model is incorporated in the framework of an incremental convex programming model developed by Mahmoud *et al.* (1993, 1998) to solve variational inequality. In section 4 we present the details of the proposed incremental procedure including: the finite element implementation, determination of the incremental size and updating the stiffness matrix by adding the contribution of friction during successive increments. The contact problem of an elastic block on a rigid foundation is solved by the proposed solution model and the results of some parametric studies are discussed in section 5.

2. The proposed friction model

To model friction phenomenon the welding-ploughing theory is employed. Due to the roughness of the contacting surfaces, actual contact occurs only at individual spots. Application of a normal force, not only increase the actual contact area but also cause local welding between the contacting spots forming individual junctions. The strength of each of these junctions is proportional to the induced normal stress σ_n at its location.

If a tangential force T is applied and increased steadily, the induced shear stress at the contact surface will continuously increase but not exceed certain level τ that cause fracture of all junctions. The application of T creates also a tendency for the two bodies to slip relative to each other. If the relation between the induced shear stress and micro-slip is assumed linear and that micro-slip

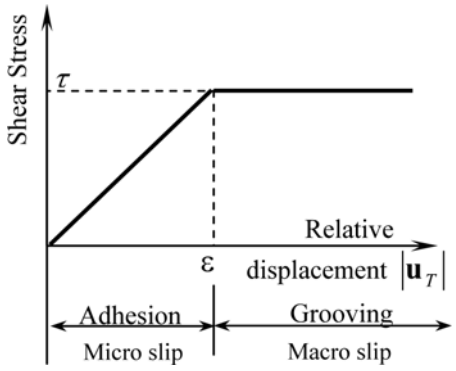

Fig. 1 Welding-ploughing model

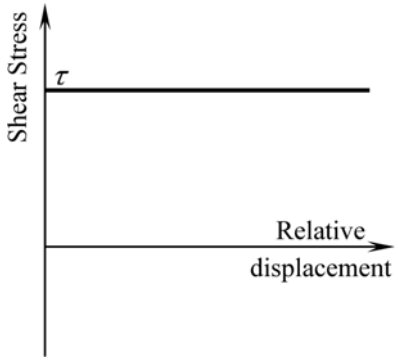

Fig. 2 Coulomb's friction model ($\varepsilon = 0$)

approaches the value ε when the critical stress τ is approached, then the parameter ε can be regarded as a measure of the stiffness of elastic junctions. When the shear stress reaches τ, grooving motion starts up with a neglected resistance (Fig. 1). In contrast, the classical Coulomb's friction model is represented in Fig. 2.

The shear stress limit τ is directly proportional to the induced normal stress σ_n, or $\tau(\mathbf{u}) = \mu|\sigma_n(\mathbf{u})|$ where μ is the coefficient of friction, $\mathbf{u}(x)$ is the displacement at location x. The nonlinear relation between the shear (frictional) stress and the tangential displacements along the contact surface can be represented as:

$$\sigma_t(u) = -\tau(u)\varphi_\varepsilon(|u_T|)\frac{u_T}{|u_T|} \tag{1}$$

where the scalar function $\varphi_\varepsilon(|\mathbf{u}_T|)$ is defined as:

$$\varphi_\varepsilon(|\mathbf{u}_T|) = \begin{cases} |\mathbf{u}_T|/\varepsilon & \text{if} \quad |\mathbf{u}_T| \le \varepsilon \\ 1 & \text{if} \quad |\mathbf{u}_T| > \varepsilon \end{cases} \tag{2}$$

3. The variational inequality formulation

Consider a linearly elastic body, which occupies a smooth bounded domain $\overline{\Omega} \subset R^2$. Its boundary Γ consists of three disjoint parts: Γ_D, Γ_F, Γ_C. On Γ_D, $\mathbf{u} = \mathbf{0}$. The body is pressed against a rigid foundation. Beside the external boundary traction $\mathbf{t}$ along Γ_F, external body force with intensity $\mathbf{f}$ is applied in Ω. Γ_C is the candidate contact region but the actual contact region is unknown a priori and is dependent on the displacement field $\mathbf{u}$ of the elastic body. The initial gap between Γ_C and the rigid foundation is represented by a smooth function g. Along Γ_C, contact conditions should ensure that the normal stress is compressive $(\sigma_n(\mathbf{u}) \le 0)$ and that the displacements satisfy the kinematical constraint $(\mathbf{u} \cdot \mathbf{n} - g) \le 0$ to prevent interpenetration, where $\mathbf{n}$ the outward unit normal to Γ_C.

The variational formulation of Signorini problem (Kikuchi and Oden 1988, Duvaut and Lions 1976, Baiocchi and Capelo 1984, Haslinger 1992, Helal 2000, Rocca and Cocu 2001) can be obtained if we consider the constrained space K of admissible displacements defined on $\overline{\Omega}$ such that: $\mathbf{v} \in K$ implies that $\boldsymbol{v} = \mathbf{0}$ on Γ_D and $\mathbf{u} \cdot \mathbf{n} - g \le 0$ on Γ_C

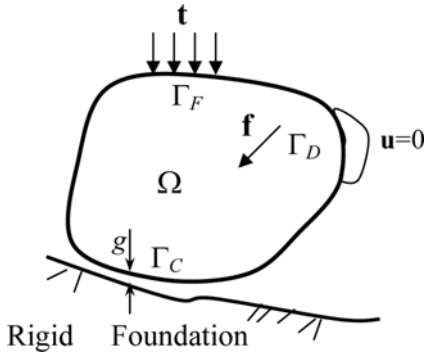

Fig. 3 An elastic body in contact with a rigid foundation

The frictional contact problem is formulated using the virtual work principle as the following variational inequality.

Find $u \in K$ such that

$$a(\mathbf{u}, \mathbf{v}-\mathbf{u}) + J_\varepsilon(\mathbf{u}, \mathbf{v}) - J_\varepsilon(\mathbf{u}, \mathbf{u}) \geq f(\mathbf{v}-\mathbf{u}) \quad \forall \mathbf{v} \in K \tag{3}$$

where

$$a(\mathbf{u}, \mathbf{v}) = \int_\Omega E_{ijkl}\mathbf{u}_{k,l}\mathbf{v}_{i,j}d\Omega \tag{4}$$

$$J_\varepsilon(\mathbf{u}, \mathbf{v}) = \int_{\Gamma_C} \tau(\mathbf{u})\,\psi_\varepsilon(|\mathbf{v}_T|)d\Gamma \tag{5}$$

$$f(\mathbf{v}) = \int_\Omega \mathbf{f}\cdot\mathbf{v}d\Omega + \int_{\Gamma_F} \mathbf{t}\cdot\mathbf{v}d\Gamma \tag{6}$$

where E_{ijkl} are elastic constants of the material, $\mathbf{u}_{k,l} = \partial\mathbf{u}_k/\partial \mathrm{x}_l$ and $\psi_\varepsilon(|\mathbf{u}_T|)$ is defined such that its derivative $\psi_\varepsilon'(|\mathbf{u}_T|)$ equals the function $\varphi_\varepsilon(|\mathbf{u}_T|)$ given by Eq. (2). Thus $\psi_\varepsilon(|\mathbf{u}_T|)$ can be constructed as:

$$\psi_\varepsilon(|\mathbf{u}_T|) = \begin{cases} \dfrac{1}{2\varepsilon}|\mathbf{u}_T|^2 & \text{if} \quad |\mathbf{u}_T| \leq \varepsilon \\ |\mathbf{u}_T| - \dfrac{\varepsilon}{2} & \text{if} \quad |\mathbf{u}_T| > \varepsilon \end{cases} \tag{7}$$

Using inequality (3) and the regularization function $\psi_\varepsilon(|\mathbf{u}_T|)$ Eq. (7), existence and uniqueness of solution of Signorini problem with friction have been addressed by Oden and Pires (1983) for a nonlocal friction law and by Rocca and Cocu (2001) for local one.

4. The proposed solution of the variational inequality

The solution procedure of variational inequality (3) starts by assuming that $\tau(\mathbf{u})$ is initially known rather than being a function of the unknown field $\mathbf{u}$. Using this assumption, the functional J_ε given by Eq. (5) depends only on one argument.

$$J_\varepsilon(\mathbf{v}) = \int_{\Gamma_C} \tau\psi_\varepsilon(|\mathbf{v}_T|)d\Gamma \tag{8}$$

Accordingly, inequality (3) can easily be put in the following constrained minimization problem

Find $\mathbf{u} \in K$ such that

$$F(\mathbf{u}) \leq F(\mathbf{v}) \qquad \forall \mathbf{v} \in K \tag{9}$$

where

$$F(\mathbf{v}) = \frac{1}{2}a(\mathbf{v}, \mathbf{v}) - f(\mathbf{v}) + J_\varepsilon(\mathbf{v}) \tag{10}$$

By obtaining the solution $\mathbf{u}$ of the minimization problem, $\tau(\mathbf{u}) = \mu\sigma_n(\mathbf{u})$ is directly computed and substituted for τ in Eqs. (8) and (10) to obtain a better minimum solution of the updated functional $F(\mathbf{v})$. Convergence of this iterative procedure has been proven in Oden and Pires (1983), Kikuchi and Oden (1988). Usually two or three of such iterations are sufficient to converge to the solution of variational inequality (3).

4.1 Solution of the constrained minimization problem

In order to solve the minimization problem defined by Eqs. (9) and (10), the Lagrangian L is constructed as:

$$\mathbf{L}(v, \Sigma) = \mathbf{F}(v) + [\Sigma, \mathbf{C}v - \mathbf{g}] \tag{11}$$

where $\Sigma \in \mathbf{G}$, $\mathbf{v} \in \mathbf{V}$, G is the space of admissible functions defined on Γ_C, $\Sigma \in \mathbf{G}$ implies that $\Sigma \geq 0$ and V is the space of admissible displacements defined on $\overline{\Omega}$ such that: $\mathbf{v} \in \mathbf{V}$ implies that $\mathbf{v} = \mathbf{0}$ on Γ_D. In Eq. (11), C is an operator such that $C\mathbf{v} = \mathbf{n} \cdot \mathbf{v}$ and $[\cdot, \cdot]$ is defined by $[\sigma, u] = \int_{\Gamma_C} \sigma \cdot u \mathbf{d}\Gamma$

Both the functional F and the contact constraints are convex and Gâteaux differentiable; it is coercive on V; then there exist a unique solution $(\mathbf{u}, \sigma) \in V \times G$, which is satisfying Kuhn-Tucker condition of minimization and characterized as the solution of the system (Kikuchi and Oden 1988):

$$\left.\begin{aligned} &\text{find } (\mathbf{u}, \sigma) \in V \times G: \\ &\quad a(\mathbf{u}, \mathbf{v}) + \langle DJ_\varepsilon(\mathbf{u}), \mathbf{v}\rangle + [\sigma, C\mathbf{v}] = f(\mathbf{v}) \quad \forall \mathbf{v} \in V \\ &\quad [\sigma - \Sigma, C\mathbf{u} - g] \geq 0 \qquad\qquad\qquad\quad \forall \Sigma \in G \end{aligned}\right\} \tag{12}$$

where

$$\langle DJ_\varepsilon(\mathbf{u}), \mathbf{v}\rangle = \int_{\Gamma_C} \tau \varphi_\varepsilon(|\mathbf{u}_T|) \frac{\mathbf{u}_T \cdot \mathbf{v}_T}{|\mathbf{u}_T|} d\Gamma \tag{13}$$

The finite element approximation of the regularized problem on the discretized domain Ω_h is characterized by:

$$\begin{aligned} &\text{find } (\mathbf{u}_h, \sigma_h) \in V_h \times G_h: \\ &\quad a(\mathbf{u}_h, \mathbf{v}_h) + \langle DJ_\varepsilon(\mathbf{u}_h), \mathbf{v}_h\rangle + [\sigma_h, C\mathbf{v}_h] = f(\mathbf{v}_h) \quad \forall \mathbf{v}_h \in V_h \\ &\quad [\sigma_h - \Sigma_h, C\mathbf{u}_h - g] \geq 0 \qquad\qquad\qquad\quad \forall \Sigma_h \in G_h \end{aligned} \tag{14}$$

where V_h and G_h are spaces of finite elements approximation for displacements and contact pressure, respectively.

The solution of Eq. (14) is still difficult due to the presence of the nonlinear term $\langle DJ_\varepsilon(\mathbf{u}_h), \mathbf{v}_h\rangle$ and the variational inequality. Between other possible iterative and incremental techniques (see for example, Zboinski and Ostachowicz 1997, Refaat and Meguid 1996, Chabrand *et al.* 2005, Klarbring 1992, Christiansen *et al.* 1998), we adopt here the application of the incremental convex programming procedure developed by Mahmoud *et al.* (1993, 1998).

4.2 The incremental procedure

This procedure has the advantage that it provides continuous information about induced stresses, deformations and development of contact versus the increase of loading. The size of load increment is chosen adaptively, such that the linearity of the system is preserved during an increment.

Let the solution $\mathbf{u}_h$, σ_h of Eq. (14) be the sum of corresponding incremental values

$$\mathbf{u}_h = \sum_{r=1}^{m} \mathbf{u}_h^{(r)}, \qquad \sigma_h = \sum_{r=1}^{m} \sigma_h^{(r)} \tag{15}$$

where $\mathbf{u}_h^{(r)}, \sigma_h^{(r)}$ are the incremental displacement vector, Lagrange multiplier in increment r, respectively and m is the total number of increments. Also, the tangential displacement vector on Γ_C can be expressed by its incremental components as follows:

$$\mathbf{u}_{hT} = u_{hT}\mathbf{T} = \left(\sum_{r=1}^{m} u_{hT}^{(r)} \right) \mathbf{T} \tag{16}$$

$\mathbf{T}$ is the unit tangent vector on Γ_C. Introducing Eq. (16) in Eq. (2), the nonlinear function $\varphi_\varepsilon(u_{hT})$ can be represented as the sum of linear scalar functions $\varphi_\varepsilon^{(r)}(u_{hT}^{(r)})$

$$\varphi_\varepsilon(u_{hT}) = \sum_{\mathbf{r}=1}^{\mathbf{m}} \varphi_\varepsilon^{(r)}(u_{hT}^{(r)}) \tag{17}$$

where

$$\varphi_\varepsilon^{(r)}(u_{hT}^{(r)}) = \begin{cases} \dfrac{u_{hT}^{(r)}}{\varepsilon} & \text{if} \quad \displaystyle\sum_{s=1}^{r-1} u_{hT}^{(s)} < \varepsilon \\ 0 & \text{if} \quad \displaystyle\sum_{s=1}^{r-1} u_{hT}^{(s)} \geq \varepsilon \end{cases} \tag{18}$$

Note that the displacement of a point in micro-slip motion is constrained by

$$0 \leq u_{hT}^{(r)} \leq \varepsilon - \sum_{s=1}^{r-1} u_{hT}^{(s)} \tag{19}$$

Introducing Eqs. (16-18) into Eq. (13), then

$$\langle DJ_\varepsilon(\mathbf{u}_h), \mathbf{v} \rangle = \sum_{r=1}^{m} b^{(r)}(\mathbf{u}_h, \mathbf{v}) \tag{20}$$

where

$$b^{(r)}(\mathbf{u}_h, \mathbf{v}) = \int_{\Gamma_C} R(\mathbf{u}_h)\mathbf{u}_{hT}^{(r)} \cdot \mathbf{v} d\Gamma \tag{21}$$

is a bilinear form and

$$R(\mathbf{u}_h) = \begin{cases} \dfrac{\tau}{\varepsilon} & \text{if} \quad \displaystyle\sum_{s=1}^{r-1} u_{hT}^{(s)} < \varepsilon \quad \text{(micro-slip)} \\ 0 & \text{if} \quad \displaystyle\sum_{s=1}^{r-1} u_{hT}^{(s)} \geq \varepsilon \quad \text{(micro-slip)} \end{cases} \tag{22}$$

A possible method for the numerical solution of the variational inequality in Eq. (14) is constructed by introducing the "slack variable" $S_h \geq 0$ such that $\sigma_h S_h = 0$ which implies: $C\mathbf{u}_h - g_h = -S_h$. Now introducing Eq. (15) yields the equivalent incremental constraints:

$$\sum_{s=1}^{r} \sigma_h^{(s)} \geq 0, \quad S_h \geq 0, \quad \left(\sum_{s=1}^{r} \sigma_h^{(s)} \right) S_h = 0, \quad C\mathbf{u}_h^{(r)} - g_h^{(r)} = -S_h \tag{23}$$

where

$$g_h^{(r)} = g_h - C \sum_{s=1}^{r-1} \mathbf{u}_h^{(s)} \tag{24}$$

Note that a point on Γ_C in contact during increment (r) is constrained by

$$S_h = 0, \quad \sum_{s=1}^{r-1} \sigma_h^{(s)} > 0, \quad \sum_{s=1}^{r} \sigma_h^{(s)} \geq 0, \text{ and hence } \sigma_h^{(r)} \geq -\sum_{s=1}^{r-1} \sigma_h^{(s)} \tag{25}$$

Also, the condition for a point on Γ_C to be separated from foundation during increment (r) is that

$$\sum_{\mathbf{s}=1}^{\mathbf{r}-1} \sigma_{\mathbf{h}}^{(\mathbf{s})} = 0, \quad \sum_{\mathbf{s}=1}^{\mathbf{r}} \sigma_{\mathbf{h}}^{(\mathbf{s})} = 0, \text{ hence } \sigma_{\mathbf{h}}^{(\mathbf{r})} = 0, \text{ and } \mathbf{S_h} \geq 0, \ \mathbf{C}u_{\mathbf{h}}^{(\mathbf{r})} \leq \mathbf{g_h} - \mathbf{C} \sum_{\mathbf{s}=1}^{\mathbf{r}-1} u_{\mathbf{h}}^{(\mathbf{s})} \tag{26}$$

Introducing Eqs. (15, 20, 23) into the minimization problem (Eq. 14), it is easy to show that a typical iteration (r) is characterized by:

$$\left.\begin{aligned} &\text{Find } (u_h^{(r)}, \sigma_h^{(r)}) \in V_h \times G_h: \\ &\quad a(u_h^{(r)}, v_h) + b^{(r)}(u_h^{(r)}, v_h) + [\sigma_h^{(r)}, Cv_h] = f_n^{(r)}(\mathrm{v}_h) \quad \forall \mathrm{v}_h \in \mathbf{V}_h \\ &\quad Cu_h^{(r)} - g_h^{(r)} = -S_h \end{aligned}\right\} \tag{27}$$

4.3 Determination of the incremental size

For each candidate node $\beta \in \Gamma_C$, the node status must be checked within an increment (r) according to the following procedure:

(1) if β is assumed to be an open node, then according to Eq. (26), $\sigma_h^{(r)}(\beta) = 0$, and the constraint $C\mathbf{u}_h^{(r)}(\beta) \leq g_h(\beta) - C\sum_{s=1}^{r-1} \mathbf{u}_h^{(s)}(\beta)$ must be an inactive one. Otherwise a fraction $M_\beta^{(r)}$ of the load can only be applied, where

$$C\mathbf{u}_h^{(r)}(\beta) M_\beta^{(r)} = g_h(\beta) - C \sum_{s=1}^{r-1} \mathbf{u}_h^{(s)}(\beta)$$

(2) if β is assumed to be a contact node, then the corresponding constraint is considered active. Therefore, according to Eq. (25), $S_h(\beta) = 0$ and the constraint $\sigma_h^{(r)}(\beta) \geq -\sum_{s=1}^{r-1} \sigma_h^{(s)}(\beta)$ must be satisfied. Otherwise the incremental load is scaled by the factor $M_\beta^{(r)}$ where

$$\sigma_h^{(r)}(\beta) M_\beta^{(r)} = -\sum_{s=1}^{r-1} \sigma_h^{(s)}(\beta)$$

(3) if β is in a micro-slip contact node, then Eq. (19) must be satisfied. Otherwise the incremental load must be scaled by

$$u_{hT}^{(r)}(\beta)M_{\beta}^{(r)} = \varepsilon - \sum_{s=1}^{r-1} u_{hT}^{(s)}(\beta)$$

For each of the above cases, if the associated constraint is fulfilled, the scale factor is set equal to 1.

The scale factor for increment (r) is defined by:

$$M^{(r)} = \operatorname{Min}_{\beta}\{M_{\beta}^{(r)}\}, \quad 0 < M^{(r)} \le 1$$

If $M^{(r)} < 1$ then only $M^{(r)}f_h^{(r)}$ can actually be applied to ensure the linearity of increment r while the remaining part $f_h^{(r+1)} = f_h^{(r)}(1 - M^{(r)})$ is to be transferred to the next increment.

4.4 The finite element discretization for an increment

Defining global basis functions $\{\Phi_{\alpha}^{h}(\mathbf{x})\}$, and $\{\eta_{\alpha}^{h}(\mathbf{x})\}$ for the displacement, and the contact pressure, respectively, then we have the following expressions for the corresponding incremental quantities. From now and up to the end of this subsection we will drop writing the increment index r for simplicity keeping in mind that these expressions represent incremental quantities

$$u_{hi}(\mathbf{x}) = \sum_{\alpha=1}^{p} u_i^{\alpha}\Phi_{\alpha}^{h}(\mathbf{x}) \quad \mathbf{x} \in \overline{\Omega}_h, \quad p \text{ is the total number of nodes in } \overline{\Omega}_h$$

$$\sigma_h(\mathbf{x}) = \sum_{\alpha=1}^{q} \sigma^{\alpha}\eta_{\alpha}^{h}(\mathbf{x}) \quad \mathbf{x} \in \overline{\Gamma}_{Ch}, \quad q \text{ is the total number of nodes in } \overline{\Gamma}_{Ch}$$

Accordingly, the bilinear forms $a(\cdot,\cdot), b(\cdot,\cdot), [\cdot,\cdot]$ and the linear form $f(\cdot)$ in Eq. (27) are given as follow:

$$a(\mathbf{u}_h, \mathbf{v}_h) = v_i^{\alpha}\tilde{E}_{\alpha\beta}^{ij}u_j^{\beta}, \quad b(\mathbf{u}_h, \mathbf{v}_h) = v_i^{\alpha}\tilde{R}_{\alpha\beta}^{ij}u_j^{\beta}, \quad [\sigma_h, C\mathbf{v}_h] = v_i^{\alpha}C_{\alpha\beta}^{i}\sigma^{\beta}$$

$$f(\mathbf{v}_h) = v_i^{\alpha}f_{\alpha}^{i} \tag{28}$$

respectively, where:

$$\tilde{E}_{\alpha\beta}^{ij} = \int_{\Omega} E_{ikjl}\Phi_{\beta,l}^{h}\Phi_{\alpha,k}^{h}d\Omega, \quad C_{\alpha\beta}^{i} = \int_{\Gamma_C} \Phi_{\alpha}^{h}n_i\eta_{\beta}^{h}d\Gamma$$

$$f_{\alpha}^{i} = \int_{\Omega} f_i\Phi_{\alpha}^{h}d\Omega + \int_{\Gamma_F} t_i\Phi_{\alpha}^{h}d\Gamma$$

$$\tilde{R}_{\alpha\beta}^{ij} = \int_{\Gamma_C} R(\mathbf{u}_h)(\delta_{ij} - n_in_j)\Phi_{\beta}^{h}\Phi_{\alpha}^{h}d\Omega \tag{29}$$

where $(\delta_{ij} - n_in_j)$ gives the projection of the unit tangent in the x, y direction.

In Eq. (28) and (29), repeated indices are summed throughout their ranges $1 \le i, j \le 2$, $1 \le \alpha, \beta \le p$ or q according to the summed component is a displacement or a stress respectively. Thus the

finite element approximation of Eq. (27) yields the discrete linear system:

$$(\tilde{E}^{ij}_{\alpha\beta} + \tilde{R}(\mathbf{u}_h)^{ij}_{\alpha\beta})u^{\beta}_{j} + C^{i}_{\alpha\beta}\sigma^{\beta} = f^{i}_{\alpha} \tag{30}$$

$$C^{j}_{\beta\alpha}u^{\beta}_{j} - g_{\alpha} = -S_{\alpha} \tag{31}$$

where $g_{\alpha} = \int_{\Gamma_C} g\,\eta^{h}_{\alpha} d\Gamma$ and $S_{\alpha} \geq 0$

Eqs. (30) and (31) can also be put in the following partitioned matrix form:

$$\begin{bmatrix} K(\mathbf{u}) & C \\ C^{T} & 0 \end{bmatrix} \begin{bmatrix} \{u\} \\ \{\sigma\} \end{bmatrix} = \begin{bmatrix} \{f\} \\ \{g - S\} \end{bmatrix} \tag{32}$$

where

$$K^{ij}_{\alpha\beta}(\mathbf{u}) = \tilde{E}^{ij}_{\alpha\beta} + \tilde{R}(\mathbf{u})^{ij}_{\alpha\beta} \tag{33}$$

is the general entry in the $2p \times 2p$ overall stiffness matrix $K(\mathbf{u})$ including the equivalent stiffness of frictional effect. Matrix C has dimension $2p \times q$ whereas each of displacement vector $\{\mathbf{u}\}$ and force vector $\{f\}$ has $2p$ components and each of the vectors $\{\sigma\}$ and $\{g - S\}$ has q components.

According to the status of contact, the set of interpenetrating constraints could be divided into active and inactive subsets. The active subset corresponds to contact points set, while the inactive subset corresponds to the non-contact set. By Eqs. (25) and (26), inactive constraint is characterized by $\sigma = 0$ while an active one is characterized by $S = 0$. So Eq. (32) can be repartitioned as:

$$\begin{bmatrix} K(\mathbf{u}) & C_A & C_N \\ C_A^{T} & 0 & 0 \\ C_N^{T} & 0 & 0 \end{bmatrix} \begin{bmatrix} \{u\} \\ \{\sigma_A\} \\ \{\sigma_N\} \end{bmatrix} = \begin{bmatrix} \{f\} \\ \{g_A\} \\ \{g_N - S\} \end{bmatrix} \tag{34}$$

where the subscripts A and N correspond to active and inactive constraints. It should be noticed that both sets of the active and inactive constraints are not known a priori. The state of each constraint could be changed from active to inactive one, and vice-versa according to the level of the applied load vector.

The effect of friction is implied in the stiffness matrix $K(\mathbf{u})$ which is a function of $\mathbf{u}$ according to (22,29,30). These equations state that incremental micro-slip against resistance with stiffness $= \tau/\varepsilon$ starts and may continue as long as the total tangential displacement is less than or equal to ε. This stiffness reduces to zero for the nodes whose total tangential displacements reach or exceed the specific value ε. Non zero contribution $\tilde{R}(\mathbf{u}_h)^{ij}_{\alpha\beta}$ occurs if α, β are adjacent nodes (or the same node) and both α and β are in micro-slip motion. For simple integration schemes, non-zero contribution occurs only on the diagonal (2×2) submatrices corresponding to nodes in micro-slip motion. If the transition from increment (r) to increment ($r + 1$) is due to the event that micro-slip motion is terminated at node α, matrix $K(\mathbf{u})$ is updated in the new increment by removing the local frictional stiffness at node α by setting $\tilde{R}(\mathbf{u}_h)^{ij}_{\alpha\beta}$ equal zero for all β.

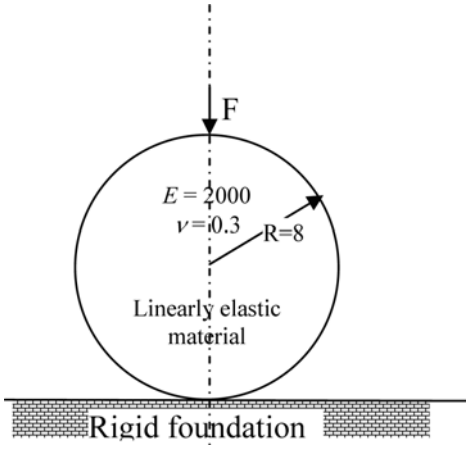

Fig. 4 The Hertiz problem

5. Numerical results

In the following numerical examples, nondimensionalized units are used and deformations may be in exaggerated scale so as to clearly exhibit features of the deformed geometry and to illustrate the proposed approach rather than solving specified contact problem.

Example 1: Hertz problem

The frictionless Hertz problem of a long circular cylinder resting on a flat foundation and subjected to a uniform load along top is considered for the purpose of comparison. It is a plane strain problem and its geometry, loading, material constants are shown in Fig. 4.

This problem has the following exact solution (Kikuchi and Oden 1988):

The half width of the contact surface b is given by:

$$b = 2\sqrt{FR(1-\nu^2)/E\pi} \tag{35}$$

and contact pressure $P(x)$

$$P(x) = \frac{2F}{\pi b^2}\sqrt{b^2 - x^2} \tag{36}$$

where x is the distance from the center line on the contact surface, R is the radius of the cylinder and F is the applied load per unit length.

The Hertz problem is solved for two different applied loads ($F = 1600$ and $F = 800$). The procedure starts by assuming that just the point at the center line is initially in contact then with the increase of load, it automatically predicts continuous extension of the contact area. The computed contact pressure distributions are compared with the exact vales in Fig. 5. Good agreement is observed for the two cases.

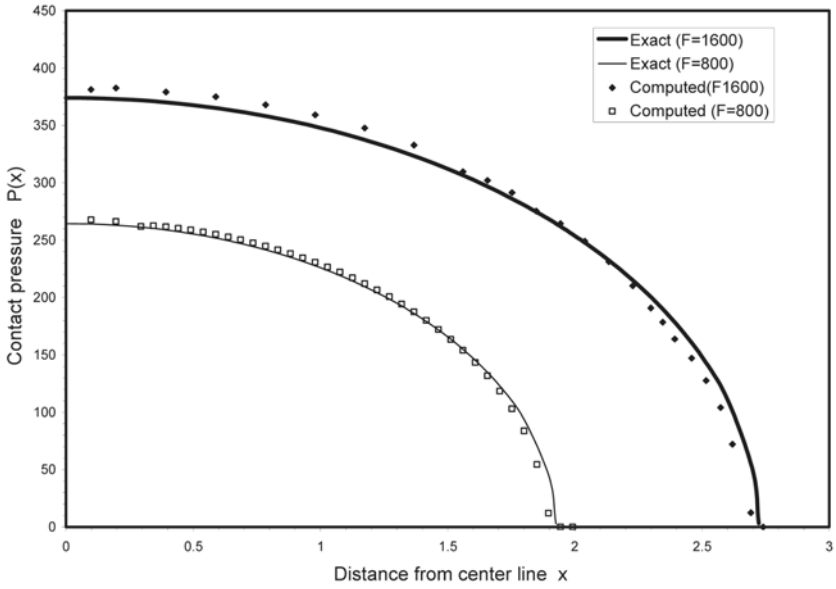

Fig. 5 Computed contact pressure distributions compared with exact ones (Kikuchi and Oden 1988) for two different values of applied loads

Example 2: Contact of an elastic block on a rigid foundation

To study the effect of the regularized parameter ε on the solution of Signorini's problems, the simple problem of an elastic block resting on a rigid foundation is solved for two different values of ε, namely $\varepsilon = 0.0001$ and $\varepsilon = 0.01$.

The block is shown in Fig. 6 and is subjected to a fixed uniform distribution of normal load P and an increasing tangential force T on the left side of the block. The material of the elastic block is homogenous with Young's modulus $E = 5 * 10^7$ (F/L^2) and Poisson's ratio $\gamma = 0.25$. The coefficient of friction is taken $\mu = 0.3$.

The evolutions of micro-slip of contact nodes according to the increase of side force T are shown in Fig. 7 and Fig. 8 for $\varepsilon = 0.0001$ and $\varepsilon = 0.01$, respectively. It is noticed that the micro-slip for the case of zero side force is symmetric in magnitude but different in direction with respect to the

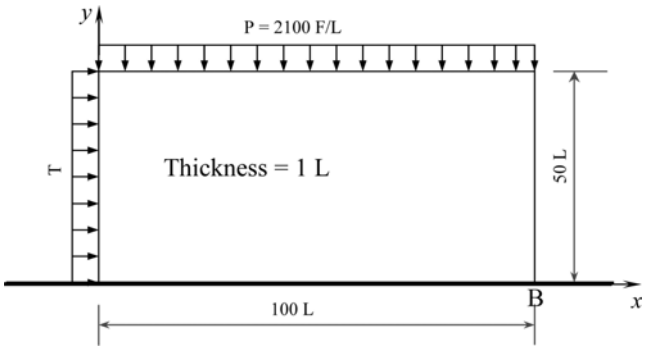

Fig. 6 An elastic block configuration

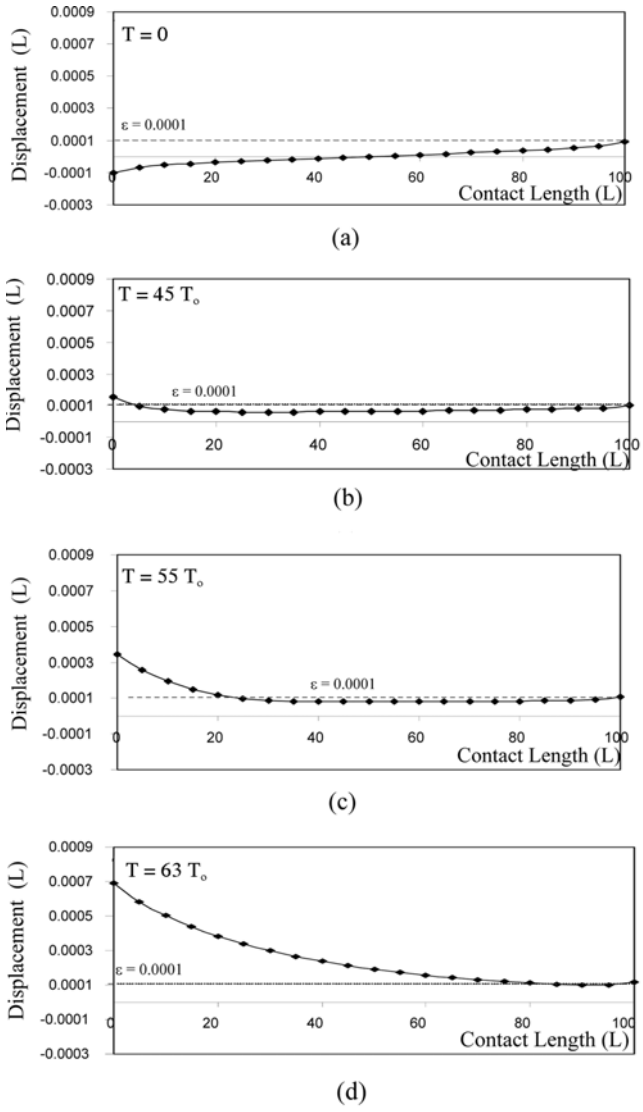

Fig. 7 Micro-slip of contacting points for different $T = kT_0$, $T_0 = 20\ F/L$ ($\varepsilon = 0.0001$)

centerline of the block; meanwhile it is noticed that the relative micro-slip of the contacting point at the centerline of the block equals zero, where no slip occurs. This is true for both values of ε (Fig. 7(a) and Fig. 8(a)). Applying the side force, the contacting points tend to slip in the forward direction (direction of the applied tangential force). We will follow the micro-slip until the global sliding of the block occurs. Global sliding takes place once all of the contacting nodes move a tangential displacement equal to or larger than the value of ε. The resultant slip due to both P and T is shown in Figs. 7(b), (c), (d). for different values of T for the case $\varepsilon = 0.0001$. These figures illustrate that a macro-slip region starts and spreads continuously until the complete sliding of the block.

For the larger value $\varepsilon = 0.01$, Figs. 8(a), (b), (c) show the tangential displacements of the

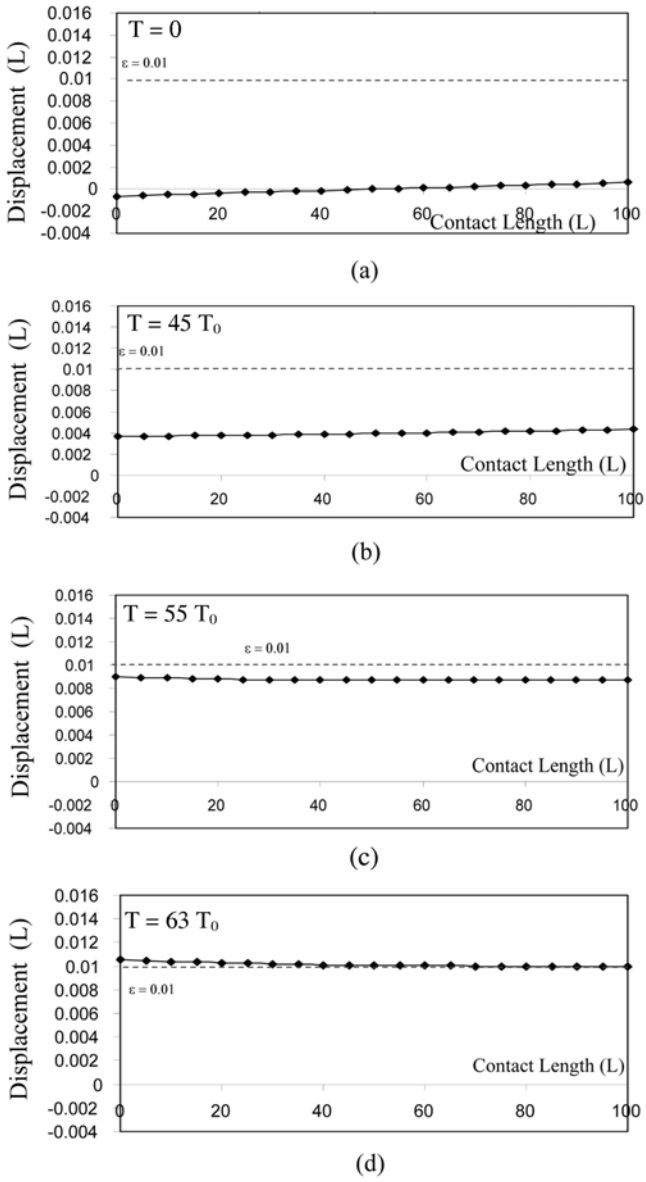

Fig. 8 Micro-slip of contacting points for different $T = kT_0$, $T_0 = 20\ F/L$ ($\varepsilon = 0.01$)

contacting points for different values of T. The figures show the increase of the slip with the increase of T. In this case, it is noticed that the slip is almost uniform for all contacting points, and hence no partial sliding region can be found, until the sudden sliding occurs.

However, we have to precisely notice that the growth of the value of ε does not affect the critical capacity of T required to make gross sliding of the body. For the two previous cases, and according to Figs. 6, 7 and 8, the value of T causing gross sliding (63 T_0 = 63(20) (50)) equals the normal force multiplied by the coefficient of friction (μP = 0,3(2100)(100)). The deformed configuration of

(a) ε = 0.0001 (b) ε = 0.01

Fig. 9 Deformed configuration of the elastic block at the instant of gross sliding

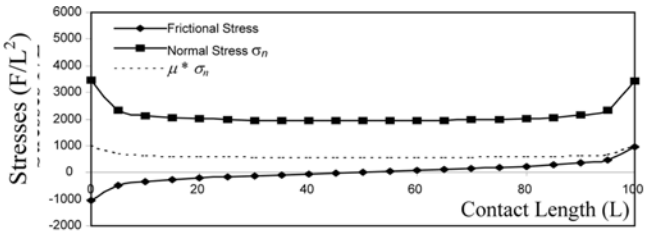

(a) T = 0

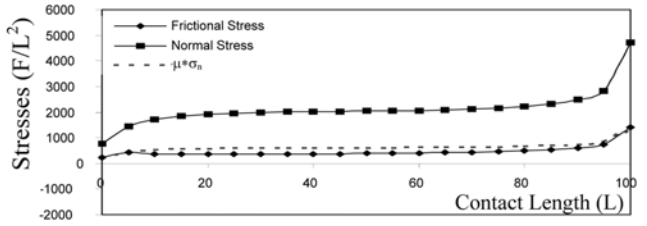

(b) T = 45 T_0

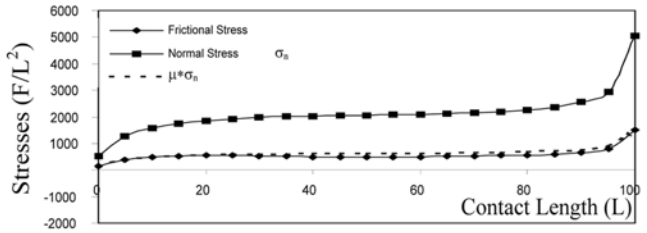

(c) T = 55 T_0

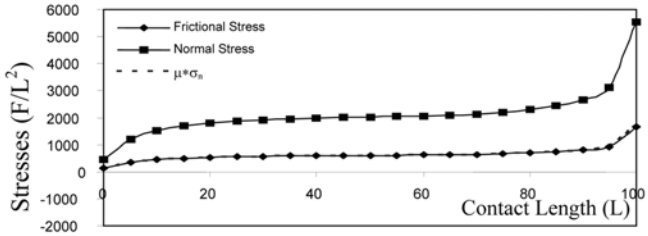

(d) T = 63 T_0

Fig. 10 Distribution of normal and frictional stresses along the contact length for different T and $\varepsilon = 0.0001$

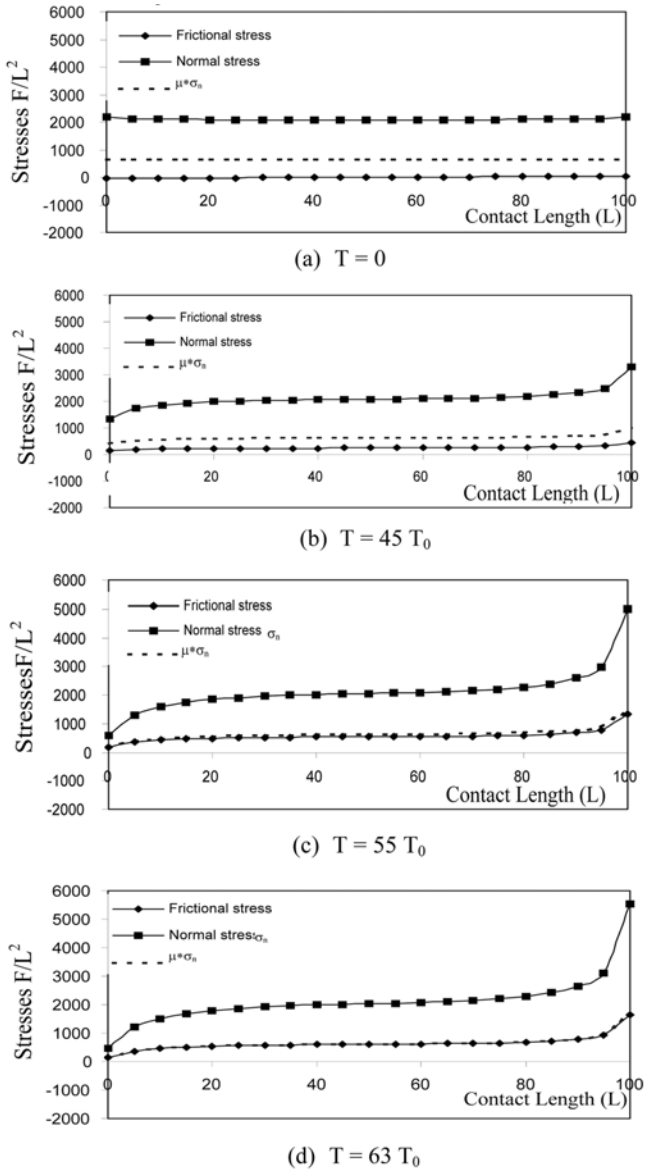

Fig. 11 Distribution of normal and frictional stresses along the contact length for different T and $\varepsilon = 0.01$

the block under the action of both P and $T = \mu P$ is represented in Fig. 9 for the two different values of ε.

Fig. 9(a) shows the computed deformed shape of the block for $\varepsilon = 0.0001$. The deformed configuration shows small tangential displacement of the contacting points with respect to the tangential displacement of points on other sides of the block. In contrast Fig. 9(b), representing the deformation at $\varepsilon = 0.01$, shows that the tangential deformation is almost uniform for all points of the block.

Contact pressure and friction stress distributions along the contact length are plotted in Fig. 10

and Fig. 11 for $\varepsilon = 0.0001$ and $\varepsilon = 0.01$, respectively. In each of these figures, a dotted curve representing the ultimate permissible tangential stress $\tau = \mu |\sigma_n|$ is plotted. Contact pressure distribution due to the normal load only is almost uniform and symmetric specially when the value of ε is relatively large (Fig. 11(a) for $\varepsilon = 0.01$). When a tangential force is applied, the contact pressure increases in the forward direction (near point B in Fig. 6) and decreases in the other. When this tangential force reaches its maximum admissible value, the contact pressure distribution seems to be independent of the value of ε, Figs. 10(d) and 11(d) show identical contact pressure distributions for the cases $\varepsilon = 0.0001$ and $\varepsilon = 0.01$, respectively.

As one would expect, the tangential stress $|\sigma_T|$ does not exceed the dotted τ curve in each of the Figs. 10 and 11. Moreover one can recognize the micro-slip region as the set of contacting points for which $|\sigma_T|$ curve lies on τ curve. Full sliding of the block occurs when the $|\sigma_T|$ curve lies completely on the τ curve. We can conclude from Fig. 10 for $\varepsilon = 0.0001$ that increasing the tangential applied force T, a macro-slip region starts at point A (see Fig. 6) and increases gradually in the forward direction to reach point B when T reaches the value μP. In Fig. 11 where $\varepsilon = 0.01$, no macro-slip region can be found until T reaches the full frictional capacity μP.

6. Conclusions

An incremental finite element model is developed to simulate the frictional contact problems. Friction effect is accounted for according to the welding-ploughing theory rather than the classical Coulomb theory. Mathematical friction model of Oden and Pires is adopted and incorporated in the framework of an incremental convex programming model developed by Mahmoud *et al.* (1993, 1998). The friction effects are accounted for as an additional tangential stiffness. The effects of the regularization parameter ε on the variation and progress of micro slip, frictional stress, and contact pressure are studied.

References

Baiocchi, C. and Capelo, A. (1984), *Variational and Quasivariational Inequalities*, John Wiley and Sons, New York.

Bowden, F.P. and Tabor, D. (1950), *The Friction and Lubrication of Solids*, Part I Clarendon Press, Oxford.

Chabrand, P., Dubois, F., Graillet, D., Boman, R. and Ponthot, J.P. (2005), "Numerical simulation of tribological devices used as a set of benchmarks for comparing contact algorithms", *J. Finite Elements in Analysis and Design*, **41**, 637-665.

Christiansen, P.W., Klarbring, A., Pang, J.S. and Stromberg, N. (1998), "Formulation and comparison of algorithms for frictional contact problems", *Int. J. Numer. Meth. Eng.*, **42**, 145-173.

Duvaut, G. and Lions, J.L. (1976), *Inequalities in Mechanics and Physics*, Springer-Verlag, Berlin.

Haslinger, J. (1992), "Signorini problem with Coulomb's law of friction. shape optimization in contact problems", *Int. J. Numer. Meth. Eng.*, **34**, 223-231.

Helal M.M. (2000), "A variational inequality model for frictional contact problems", Ph.D. Thesis, Zagazig University.

Kikuchi, N. and Oden, J.T. (1988), "Contact problems in elasticity: A study of variational inequalities and finite element methods", SIAM, Philadelphia.

Klarbring, A. (1992), "Mathematical programming and augmented Lagrangian methods for frictional contact problems", in *Proc. Contact Mechanics International Symposium,* A. Curnier, ed., PPUR, Lausanne, Switzerland.

Mahmoud, F.F., Ali-Eldin, S.S., Hassan, M.M. and Emam, S.A. (1998), "An incremental mathematical programming model for solving multi-phase frictional contact problems", *Comput. Struct.*, **68**(6), 567-581.
Mahmoud, F.F., Alsaffar, A.K. and Hassan, K.A. (1993), "An adaptive incremental approach for the solution of convex programming models", *Mathematics and Computers in Simulation*, **35**, 501-508.
Oden, J.T. and Pires, E.B. (1983), "Nonlocal and nonlinear friction laws and variational principles for contact problems in elasticity", *J. Appl. Mech.*, **50**, 67-76.
Refaat, M.H. and Meguid, S.A. (1996), "A novel finite element approach to frictional contact problems", *J. Numer. Meth. Eng.*, **39**, 3889-3902.
Rocca, R. and Cocu, M. (2001), "Existence and approximation of a solution to quasistatic signorini problem with local friction", *J. Eng. Sci.*, **39**, 1233-1255.
Zboinski, G. and Ostachowicz, W. (1997), "A general FE computer program for 3D incremental analysis of frictional contact problems of elastoplasticity", *J. Finite Elements in Analysis and Design,* **27**, 307-322.

Notation

ε	: regularization parameter for the tangential stress-displacement relation at the contact surface.
τ	: ultimate permissible tangential stress.
$\varphi_\varepsilon(x)$, $\psi_\varepsilon(x)$	: scalar functions representing the proposed friction model and such that $\frac{d\psi_\varepsilon(x)}{dx} = \varphi_\varepsilon(x)$
S, S_h	: slack variables used to represent inequalities as equations.